

Automatic *P*-Wave Arrival Detection and Picking with Multiscale Wavelet Analysis for Single-Component Recordings

by Haijiang Zhang, Clifford Thurber, and Charlotte Rowe*

Abstract We have developed an automatic *P*-wave arrival detection and picking algorithm based on the wavelet transform and Akaike information criteria (AIC) picker. Wavelet coefficients at high resolutions show the fine structure of the time series, and those at low resolutions characterize its coarse features. Primary features such as the *P*-wave arrival are retained over several resolution scales, whereas secondary features such as scattered arrivals decay quickly at lower resolutions. We apply the discrete wavelet transform to single-component seismograms through a series of sliding time windows. In each window the AIC autopicker is applied to the thresholded absolute wavelet coefficients at different scales, and we compare the consistency of those picks to determine whether a *P*-wave arrival has been detected in the given time window. The arrival time is then determined using the AIC picker on the time window chosen by the wavelet transform. We test our method on regional earthquake data from the Dead Sea Rift region and local earthquake data from the Parkfield, California region. We find that 81% of picks are within 0.2-sec of the corresponding analyst pick for the Dead Sea dataset, and 93% of picks are within 0.1 sec of the analyst pick for the Parkfield dataset. We attribute the lower percentage of agreement for the Dead Sea dataset to the substantially lower signal-to-noise ratio of those data, and the likelihood that some percentage of the analyst picks are in error.

Introduction

Quickly detecting and accurately picking the first *P*-wave arrival is of great importance in event location, event identification, and source mechanism analysis, especially in the era of large volumes of digital and real-time seismic data. Manual analysis of seismograms and phase picking is time-consuming and subjective. There is a need to provide a more efficient alternative.

Various techniques have been presented in the literature for detecting and picking the arrivals of different seismic waves from single-component as well as three-component (3-C) recordings. Because some seismic stations cannot provide consistent 3-C signals, it is important to be able to pick seismic arrivals from single-component recordings. Withers *et al.* (1998) have categorized previous trigger algorithms for onset picking into time domain, frequency domain, particle motion processing, or pattern matching. Some of the current methods include energy analysis (Earle and Shearer, 1994), polarization analysis (Vidale, 1986), and autoregressive techniques (Maeda, 1985; Sleeman and Eck, 1999; Leonard and Kennett, 1999; Leonard, 2000).

Autoregressive techniques are based on the assumption that the seismogram can be divided into locally stationary segments as an autoregressive (AR) process and the intervals before and after the onset are two different stationary processes (Sleeman and Eck, 1999). On the basis of this assumption, an autoregressive-Akaike information criteria (AR-AIC) method has been used to detect *P* and/or *S* phases (Sleeman and Eck, 1999; Leonard and Kennett, 1999; Leonard, 2000). For the AR-AIC picker, the order of the AR process must be specified by trial and error and the AR coefficients have to be calculated for both intervals. In contrast to the AR-AIC picker, Maeda (1985) uses a different AIC picker, which can be calculated directly from the records without fitting them with the AR processes. However, when the signal-to-noise ratio (S/N) is low and the arrival is not evident, the AIC picker does not perform well. Further, for the AIC picker to identify the proper arrival, a limited time window of the data must be chosen.

We present an application of the wavelet transform to guide the work of the AIC picker. The wavelet transform has been used to detect and pick the arrival of several seismic phases. Anant and Dowlal (1997) applied the discrete wavelet transform (DWT) to 3-C seismograms to identify the *P*-

*Present address: EES-11, M.S. D408, Los Alamos National Laboratory, Los Alamos, New Mexico 87545.

and S-phase arrivals of seismic events by using the polarization and amplitude information contained in the wavelet coefficients of the signals. Tibuleac and Herrin (1999) used the continuous wavelet transform to decompose the Lg signal into different scales, and applied a threshold detector to the wavelet coefficients at one scale to determine the Lg arrival time. Gendron *et al.* (2000) jointly detected and classified seismic events via Bayes theorem by using features extracted from wavelet coefficients of the records.

The wavelet transform decomposes the signal at different scales, thus adaptively characterizing its components at different resolutions. The primary features in the signal (phase arrivals) are retained over several resolution scales and irrelevant ones (noise) decay quickly at larger scales (Daubechies, 1992), although we note that some seismic noise will also be present at larger scales (e.g., microseisms). We apply thresholding to the wavelet coefficients using the Birge-Massart penalization method to denoise the seismogram (Birge and Massart, 1997). Then the AIC picker is used on the penalized wavelet coefficients over multiple scales. By comparing the consistency among the picks at different scales, we can determine whether there is an arrival in the current time window. After a time window is chosen, we apply the AIC autopicker to the denoised signal reconstructed from the thresholded wavelet coefficients to determine the arrival time. We test our method on regional earthquake data from Dead Sea Rift region and local earthquake data from Parkfield, California region, and compare the autopicks with analyst picks.

AIC Picker

For the standard AR-AIC approach, it is assumed that a seismogram can be divided into locally stationary segments, each modeled as an AR process, and that the intervals before and after the onset time are two different stationary processes (Sleeman and van Eck, 1999). Either the order of the AR process or values of the AR coefficients or both will change when the characteristics of the current segment of the seismogram are different from those of the previous one. For example, typical seismic noise is well represented by a relatively low-order AR process, whereas seismic signals gradually require a higher-order AR process (Leonard and Kennett, 1999). The AIC is usually used to determine the order of the AR process when fitting a time series, which indicates the badness and the unreliability of the model fit (Akaike, 1973). This method has been used in onset estimation by analyzing the variation in AR coefficients representing both multicomponent and single-component traces of broadband and short-period seismograms (Leonard and Kennett, 1999). When the order of the AR process is fixed, the AIC function is a measure of the model fit. The point where the AIC is minimized in the least-squares sense determines the optimal separation of the two stationary time series, and thus is interpreted as the phase onset (Sleeman and Eck, 1999). This approach is known as AR-AIC picker (Sleeman and Eck,

1999; Leonard, 2000). The AIC of the two-interval model for seismogram x of length N is represented as function of merging point k (Sleeman and Eck, 1999):

$$\text{AIC}(k) = (k - M)\log(\sigma_{1,\max}^2) + (N - M - k)\log(\sigma_{2,\max}^2) + C_2 \quad (1)$$

where M is the order of an AR process fitting the data, C_2 is a constant, and $\sigma_{1,\max}^2$ and $\sigma_{2,\max}^2$ indicate the variance of the seismogram in the two intervals not explained by the autoregressive process. To realize the AR-AIC picker, the order of the AR process must be specified by trial and error, and then AR coefficients can be determined by the Yule-Walker equations (Haykin, 1996).

In contrast to the AR-AIC picker, Maeda (1985) calculates the AIC function directly from the seismogram, without using the AR coefficients. The onset is the point where the AIC has a minimum value. For the seismogram x of length N , the AIC value is defined as

$$\text{AIC}(k) = k \cdot \log\{\text{var}(x[1,k])\} + (N - k - 1) \cdot \log\{\text{var}(x[k + 1,N])\} \quad (2)$$

where k ranges through all the seismogram samples.

The AIC picker defines the onset point as the global minimum. For this reason, it is necessary to choose a time window that includes only the seismogram segment of interest. If the time window is chosen properly, the AIC picker is likely to find the P -wave arrival accurately. For a seismogram with a very clear onset, AIC values have a very clear global minimum that corresponds to the P -wave arrival (Fig. 1a). For a seismogram with a relatively low S/N ratio, there may be several local minima in AIC values, but the global minimum still indicates accurately the P -wave onset (Fig. 1b). When there is more noise than signal in the seismogram, the global minimum cannot be guaranteed to indicate the P -wave arrival (Fig. 1c). Thus, the S/N ratio in the seismogram affects the accuracy of the AIC picker to some extent.

If there are multiple seismic phases in a time window, the AIC picker will choose the strongest phase (Fig. 2). On the other hand, because there will almost always be one global minimum in a time window, the AIC picker will usually pick an “onset” for any segment of data no matter whether there is a true phase arrival or not (Fig. 3). For this reason, we need to guide the work of the AIC picker by choosing an appropriate time window for it.

Wavelet Transform

The Fourier transform is conventionally used to analyze the frequency content of seismic signals. Fourier analysis gives a global representation of the data but cannot analyze its local frequency content or its regularity. (If the m th derivative of the signal resembles $|x - x_0|^m$ locally around x_0 ,

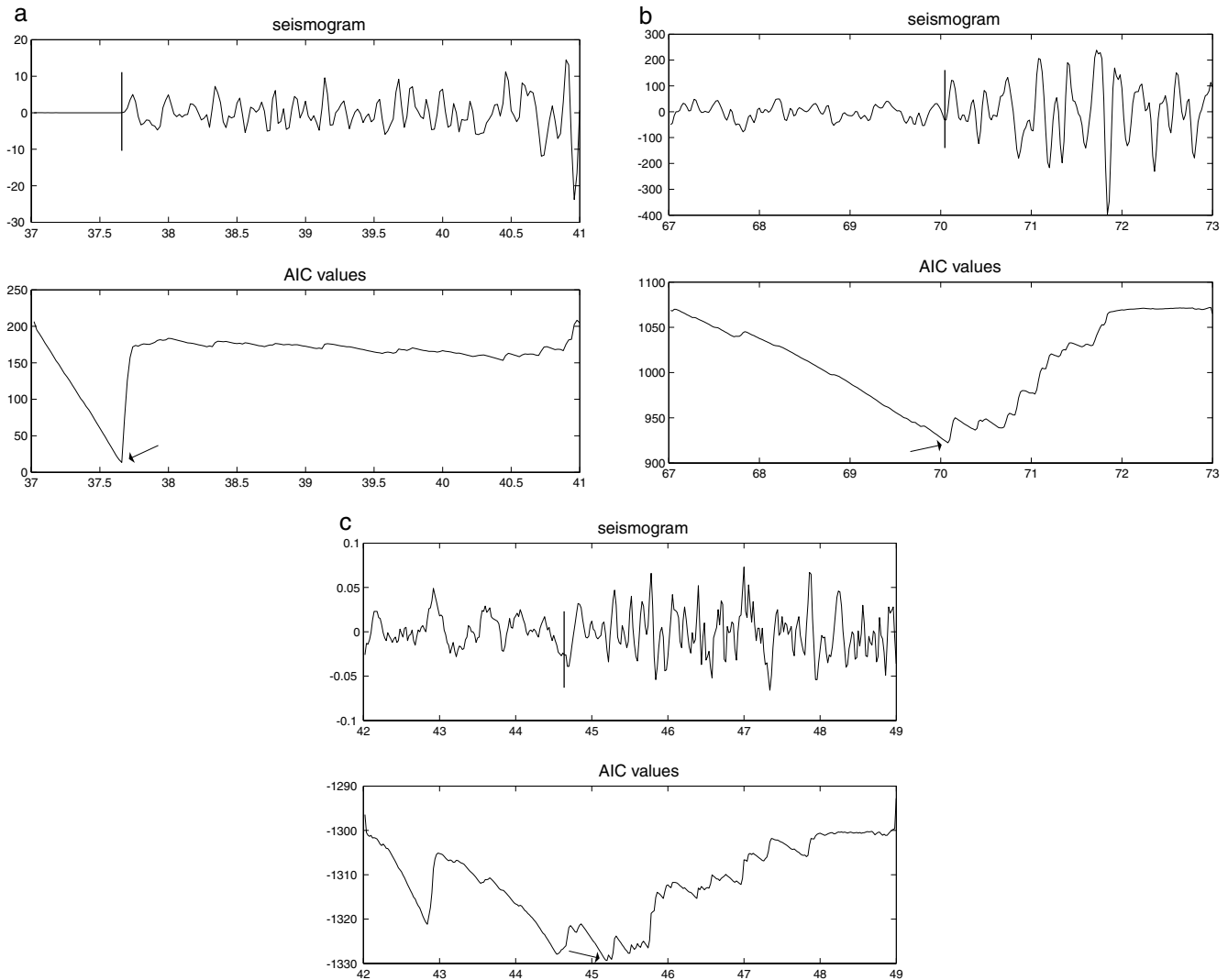


Figure 1. Seismograms and their corresponding AIC values. (a) For a seismogram with a very clear P -wave arrival (indicated by a thick line), the AIC value is a very clear minimum point (indicated by an arrow). (b) For a seismogram with a rather clear P -wave arrival but with relatively lower S/N ratio, the AIC function has many local minima, whereas the global minimum (arrow) still corresponds to the P -wave onset. (c) For a very low S/N seismogram, there are a few local minima close to each other. In this case, the global minimum (arrow) cannot be guaranteed to be the P -wave arrival.

then the regularity $p = m + r$ with $0 < r < 1$. The signal is more regular with greater p .)

Because seismic waves traveling through complex media are composed of time-frequency-localized waveforms, it is better to choose a basis that can represent the seismogram locally both in the time and frequency domains. The wavelet transform, which was actually initiated by work on seismic signals (Goupillaud *et al.*, 1984; Grossmann and Morlet, 1984), is a very useful tool in the analysis of such nonstationary signals. The advantage of the wavelet transform over the Fourier transform is its ability to characterize the structure of the signal locally with a detail matched to its scale, that is, coarse (low frequency) features on large scales and fine (high frequency) features on small scales.

The wavelet transform has been used in several applications such as improving the seismic data resolution and its S/N ratio (Chakra and Okaya, 1995), compressing seismic data (Lervik *et al.*, 1996), characterizing the singularity structure of media (Goudswaard and Wapenaar, 1998), and seismic data inversion and migration (Wu and McMechan, 1998). It has also been used to detect P - and S -wave arrivals in 3-C seismograms (Anant and Dowla, 1997), to determine arrival times of the regional phase Lg (Tibuleac and Herrin, 1999), and to detect and classify seismic events (Gendron *et al.*, 2000).

The wavelet transform has two forms: continuous wavelet transform (CWT) and DWT (Daubechies, 1992). The CWT of a function $x(t)$ is defined as:

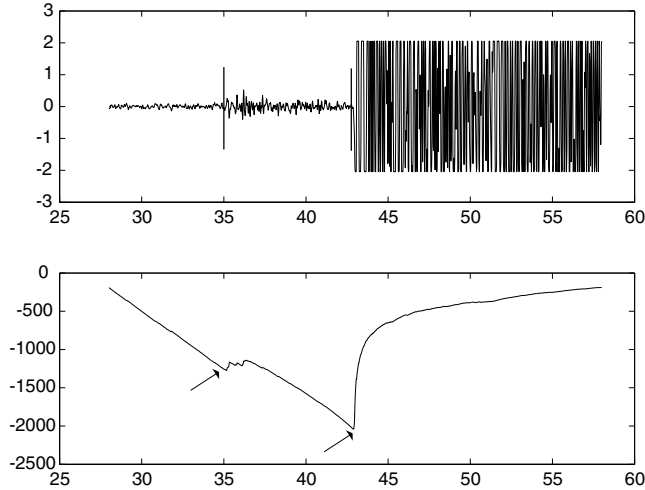


Figure 2. Seismogram with two phases and their corresponding AIC values. There are clear local minima (indicated by arrows) with respect to each phase arrival (indicated by a thick line). The global minimum indicates the arrival of the stronger phase.

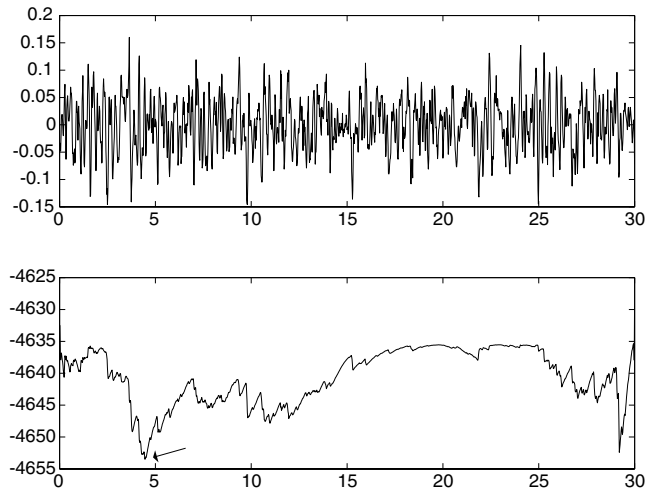


Figure 3. Seismic noise data and their AIC values. The minimum value (indicated by an arrow) does not indicate any phase arrival although it divides the data into two different stationary segments.

$$W(a, b) = \frac{1}{\sqrt{a}} \int_{-\infty}^{\infty} x(t) g\left(\frac{t-b}{a}\right) dt \quad (3)$$

where $g(t)$ is the analyzing wavelet, and a and b are the scale and translation factors, respectively. The analyzing wavelet $g(t)$ decays rapidly to zero with increasing t and has zero mean. The domain (range) of nonzero values of the wavelet is known as the support, denoted here by K . The scale factor controls the dilation or compression of the wavelet. At lower scales, the wavelet is compressed and characterizes the rapidly changing details of the signal, whereas at higher scales,

the wavelet is stretched over a greater time span and the slowly changing and coarse features are better resolved.

In practical applications, the DWT is preferred because waveforms are recorded as discrete time samples. DWT can be implemented quickly via the Mallat algorithm (Mallat, 1989). A low-pass filter h and high-pass filter g are used to calculate recursively the wavelet coefficients $\{d^1, d^2, \dots\}$ of a discrete time series s^0 , as follows

$$\begin{aligned} s^{j+1}(k) &= \sum_l h(l-2k) s^j(l) \\ d^{j+1}(k) &= \sum_l g(l-2k) s^j(l) \end{aligned} \quad (4)$$

$$j = 0, \dots, J-1$$

where k and l are the sample indexes, j is the scale parameter, and J is the maximum decomposition level. Through the decomposition, the original signal s^0 can be represented as $\{d^1, d^2, \dots, d^J, s^J\}$ from which the original signal can be reconstructed completely (Daubechies, 1992). The wavelet coefficients $\{d^1, d^2, \dots\}$ characterize the details, or the fine structure of the signal, at different scales, or resolutions. The coefficients $\{s^1, s^2, \dots\}$ represent the approximations of the signal at different scales. In a sense, the s^j coefficients indicate the residuals of the signal after the high-frequency components at lower scales are removed. In this way, we can analyze the signal at different resolutions.

Singularity Detection with Multiscale Wavelet Analysis

A singularity at a particular point of a signal is defined as a discontinuity in the signal or its derivatives at that point, which is often characterized by the local Lipschitz exponent α (Mallat and Hwang, 1992). For example, signal edges have zero Lipschitz exponents and regular signals possess positive Lipschitz exponents, whereas Gaussian noise usually has a negative one.

The change of the absolute wavelet coefficients over scales depends on the local singularity of the signal (Mallat and Hwang, 1992; Hsung *et al.*, 1999). When a point of a signal has a negative Lipschitz exponent, the corresponding absolute wavelet coefficients inside the corresponding ‘‘cone of influence’’ (COI) decay as the scale increases, where the COI is the support of the wavelet function at different scales. The radius of this cone is less than or equal to the product $K * 2^j$, where K is the support and j is the scale (Fig. 4a). However, the absolute wavelet coefficients corresponding to regular signals and signal edges increase or remain the same as the scale increases. That is, the significant features in the signal are retained over several scales, whereas random noise or other incoherent features will disappear at larger scales. On the basis of such interscale features of wavelet coefficients, the noise and the signal can be separated. Usually, a P -wave arrival is characterized by a rapid change in amplitude and/or the arrival of high-frequency or broad-band en-

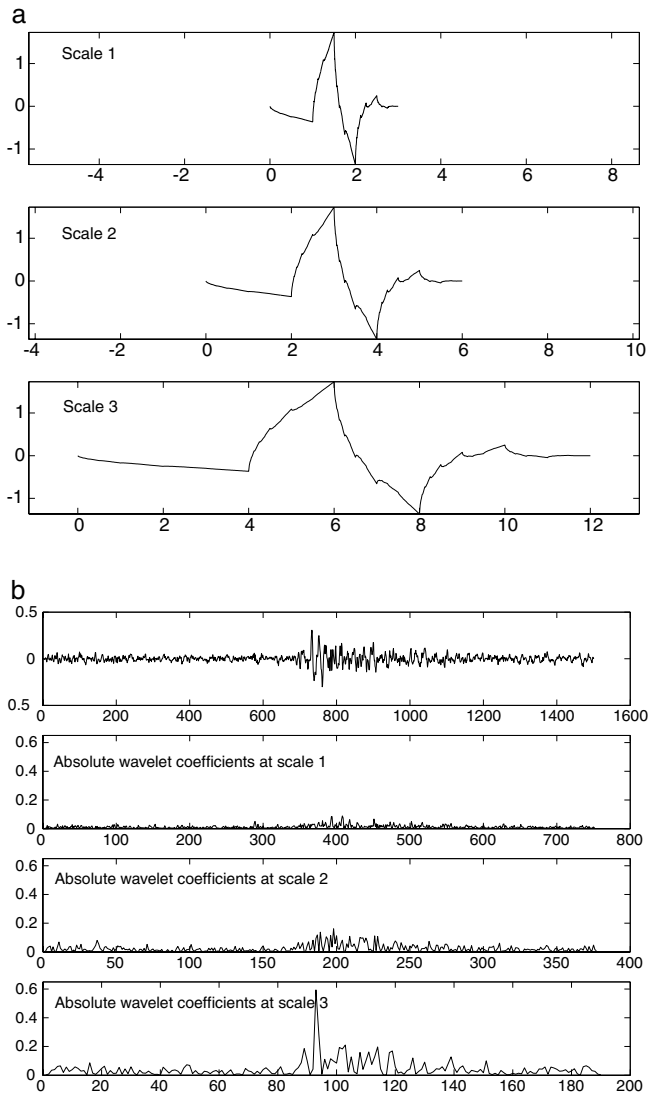


Figure 4. (a) Cone of influence (COI) of the Daubechies wavelet of order 2 (Dau2) at scales 1, 2, and 3. (b) Seismogram and the corresponding absolute wavelet coefficients using Dau2 wavelet at scales 1, 2, and 3.

ergy. It usually has a positive or at least zero Lipschitz exponent and will be retained across several scales. This property allows the *P*-wave arrival to be detected. Figure 4b shows a noisy seismogram and its corresponding wavelet coefficients at scales 1, 2, and 3. The absolute wavelet coefficients corresponding to the *P*-wave arrival increase rapidly, whereas those of the noise or secondary features decrease or (in this case) increase more slowly with increasing scale.

Wavelet-AIC Picker

Detecting and Picking the *P*-Wave Arrival

Our wavelet-AIC (W-AIC) picker combines the AIC picker with multiscale wavelet analysis, in which the AIC

picker is applied to absolute wavelet coefficients at several scales (or resolutions). If *P*-wave arrival information is retained over several scales, the times picked by the AIC picker at several scales should be in close proximity to one another (Fig. 5a–c). If there is no *P*-wave arrival within a time window, there will be significant differences between the pick times at neighboring scales (Fig. 5d). By this method, we can determine whether there is a *P*-wave arrival. Table 1 lists pick times at three scales as well as manual picks, if applicable, for the seismograms shown in Figure 5. We have found that decomposing the seismograms into three scales is appropriate. If more scales are used, the COIs of those singularities that are not isolated will have more overlap and cause more ambiguities. If only two scales are used, however, the singularity due to the noise will still be significant at scales 1 and 2 in some cases, resulting in too many false detections.

There are numerous wavelet families from which to choose. The main criteria for choosing the wavelet function are its support, symmetry, regularity, and number of vanishing moments (Wickerhauser, 1994). The wavelet function with tighter support has smaller border distortion of the DWT and COI. In general, short wavelets are often more effective than long ones in detecting a signal singularity. So to detect a signal discontinuity, the best choice is to use the Harr wavelet, which has the support of only 2. However, it fails to detect a singularity in the j th ($j > 0$) derivative. Instead, the wavelet used should be sufficiently regular with at least j vanishing moments.

For the seismogram shown in Figure 5a, we use several wavelet functions from the Matlab Wavelet Toolbox 2.2 to test the pick times at scales 1, 2, and 3. The results are shown in Table 2. For the same wavelet, the pick times at different scales are within 16 samples or 0.32 sec, indicating that there is a significant feature in this time window. It is noted that the Symmlet wavelet functions (symmetric Daubechies wavelets) give the same pick times at scales 1, 2, and 3 as those given by the Daubechies nonsymmetric wavelets. Pick times at different scales for other wavelets vary somewhat. This indicates the effect of the COI, and demonstrates that the wavelet coefficients cannot characterize the exact position of a singularity, but a region of the singularity (Mallat and Huang, 1992; Wickerhauser, 1994). For this reason, we use the wavelet detector to determine whether there is a *P*-wave arrival in the current time window and adopt the pick at scale 2 as the preliminary pick. Then the conventional AIC picker is used on the seismogram segment chosen on the basis of the preliminary pick.

In our test using the Daubechies wavelet of order 2 (Dau2), whose support is 4, the maximum radii of COI at scales 1, 2, and 3 are 8, 16, and 32, respectively. Thus we assume that picks at scale 1 and scale 2 within 24 samples and picks at scale 2 and scale 3 within 48 samples are consistent. Note that this criterion gives the worst-case scenario that the theory allows. In practice, the COI may be quite small.

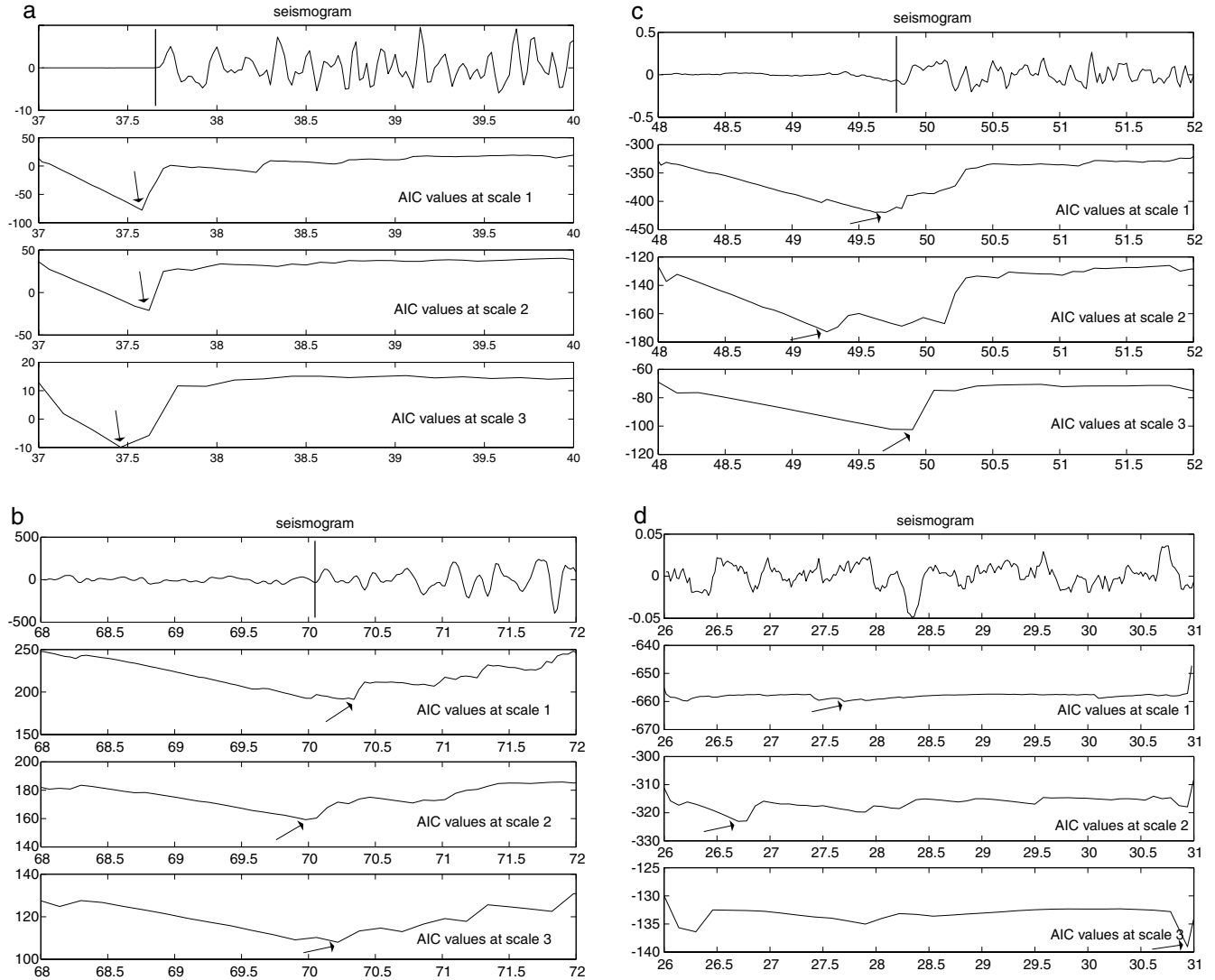


Figure 5. W-AIC picker. For seismograms shown in a, b, and c, with a *P*-wave arrival, picks at different scales are near each other. Seismogram d does not have an arrival, therefore the picks are different. *P*-wave arrival is indicated by a thick line, and picks at different scales are indicated by arrows.

When the S/N ratio is low, the W-AIC picker based on the raw wavelet coefficients usually detects and picks an incorrect arrival time. For this reason, we penalize the wavelet coefficients by soft thresholding, which has a better mathematical property than hard thresholding (Donoho, 1995). (Let t denote the threshold. The hard threshold signal is x if $|x| > t$, and is 0 if $|x| \leq t$. The soft threshold signal is $\text{sign}(x)(|x| - t)$ if $|x| > t$ and is 0 if $|x| \leq t$.) The threshold t is chosen by a wavelet coefficients selection rule using a penalization method (Birge and Massat, 1997). The W-AIC picker detects the *P*-wave arrival based on the thresholded wavelet coefficients, from which the denoised signal can be reconstructed for the AIC autopicker to pick a time. For the seismogram shown in Figure 5a, the pick time with the AIC picker is 37.64 sec, which is exactly the same as the manual pick. In comparison to conventional bandpass filtering, this

denoising scheme based on the wavelet transform decreases the distortion of the *P*-wave arrival and reduces its amplitude to a lesser extent (Fig. 6).

Implementation Details

The principle purpose of using the wavelet transform is to guide the work of the AIC picker by choosing an appropriate time window for it, in which a *P*-wave arrival exists. The time window is chosen automatically via a trial-and-error process. First, a preliminary time window is chosen and pick times at scale 1, 2, and 3 are checked to see if they are consistent. If so, the wavelet detector claims there is a *P*-wave arrival in this time window and chooses the pick time at scale 2 as the preliminary pick. If not, the time window will continue to move until a *P*-wave arrival is detected or a predefined ending time is met. After a *P*-wave arrival

Table 1
Pick Times at Scales 1, 2, and 3 and Manual Picks (a–d,
respectively) for Seismograms shown in Figure 5
(with “Dau3” Wavelet)

	a	b	c	d
Scale 1	37.58	70.34	49.70	27.70
Scale 2	37.58	69.98	49.26	26.70
Scale 3	37.58	70.22	49.90	30.94
Manual Pick	37.64	70.06	49.80	N/A

is detected, the AIC picker will pick an onset within the time segment around the preliminary pick. There are two additional aspects to consider when implementing a W-AIC picker, as follows.

Time Window. The time window for conducting the wavelet analysis is important for finding the correct phase arrival for the W-AIC picker. If the time window is too large, it may include many phases that could dominate the signal and result in a spurious pick. If the time window is too short, it will slow the detection process because neighboring time windows need to overlap to reduce the border effect. Our W-AIC picker allows the user to choose the starting and ending times for the sliding time windows. If the user does not select a windowing time, the algorithm will begin windowing from the first sample of the seismogram (with a default window length of 10 sec) until an arrival is detected.

Border Effect of the Wavelet Transform. The basic algorithm for the DWT is based on a simple scheme: convolution and downsampling. When the convolution is performed on finite-length signals, there will be border distortion, that is, there are not enough data points available near the border to conduct the convolution. The simple way to deal with border distortion is to extend the signal on both sides, such as by zero-padding, smooth padding, periodic extension, or boundary value replication methods (Strang and Nguyen, 1996). However, these methods will create some significant features (discontinuities) at both ends of the signal. For example, zero padding produces an edge singularity at both ends. Compared with the singularity of the noise, these singularities will be retained across several scales and thus be detected by the W-AIC picker. In fact, the pick times at scales 2 and 3 for the seismogram shown in Figure 5d are due to such artifacts. To circumvent this problem, we define a

border-effect region at both ends of the time window. When the time pick at some scale lies within this region, we assume it is an artifact and the pick is rejected. Time windows are overlapped so that improperly rejected arrivals may be detected in adjacent windows.

Application of W-AIC picker

We have tested the W-AIC picker in comparison with manual picks for two sets of seismic events, from the Dead Sea region (460 seismograms) and the Parkfield, California region (1112 seismograms). The earthquakes in the Dead Sea region have epicentral distances less than 300 km and magnitudes from M 0.5 to M 4.2. For the Parkfield dataset, most of the earthquakes are within 25 km of the stations and have magnitudes less than M 2.0.

We used Daubechies wavelet of order 2 (Dau2) to decompose the seismograms into three scales. If the pick times at scale 1 and scale 2 were within 24 samples and those at scale 2 and scale 3 within 48 samples, and picks at scales 1, 2, and 3 were also not within 8, 16, and 24 samples from either end of the time window, respectively (border effect), the W-AIC picker declared that a P -wave arrival existed in the time window. The pick at scale 2 was chosen as the preliminary pick. If no P -wave arrival was detected, the time window was shifted to the right with an overlap of 50 samples, continuing until the end of the seismogram (or a predefined time) was reached. After the P -wave arrival was detected, the AIC picker picked an onset within a time window of 30 samples (0.6 sec for Dead Sea dataset and 0.3 sec for Parkfield dataset) before and 50 samples (1.0 sec for Dead Sea dataset and 0.5 sec for Parkfield dataset) after the preliminary pick.

Figure 7a and b shows examples of arrivals picked by our picker for seismograms from the Dead Sea region with high S/N ratio and low S/N ratio, respectively. In both cases, the W-AIC picker detected and picked the P -wave arrival with considerable accuracy in that the picks are within 0.1 sec of analyst picks. For the Dead Sea dataset, our picker detected and picked about 80% of P arrivals correctly, among which about 81% are within 0.2 sec of manual picks. The mean value and the standard deviation of the differences between the autopicks and the manual picks are 0.052 and 0.15 sec, respectively. For the Parkfield dataset, more than 90% of picks are detected and picked within 0.5 sec of manual picks, among which about 93% are within 0.1 sec of

Table 2
The Pick Time at Scales 1, 2, and 3 with Different Wavelets for the Seismogram Shown
in Figure 5a

Wavelet	Haar	Dau2	Sym2	Sym3	Coif2	Rbio2.2	Bior2.2
Scale 1	37.58	37.58	37.58	37.58	37.62	37.58	37.62
Scale 2	37.50	37.58	37.58	37.58	37.66	37.58	37.58
Scale 3	37.42	37.42	37.42	37.58	38.00	37.58	37.58

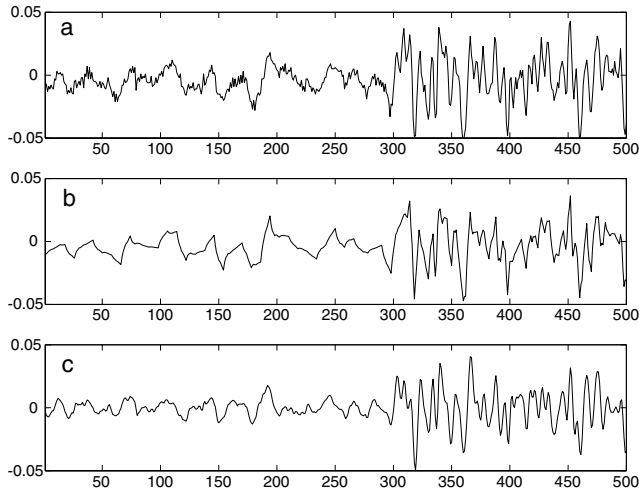


Figure 6. Comparison of wavelet denoising and bandpass-filtering methods. (a) Noisy seismogram. (b) Denoising by soft-thresholding the wavelet coefficients with the threshold chosen by the Birge-Massat method. (c) Bandpass filtering using a Butterworth filter of 1.5–10.0 Hz.

manual picks. The mean value and the standard deviation between the autopicks and manual picks are -0.002 and 0.063 sec, respectively.

We can account for the difference in results between the Dead Sea and Parkfield datasets. For the Dead Sea, the events and stations are distributed over a wide area, and the events also have a wide range of magnitudes. Therefore, the S/N ratio and the waveform characteristics are highly variable. As a result, both the analyst and the autopicker can be expected to make a relatively large number of errors. In contrast, the Parkfield dataset consists of events and stations from a very localized area, so that arrivals are on average more impulsive and waveforms are generally more similar. This leads to fewer picking errors both by the analyst and by the autopicker.

We also performed the conventional STA/LTA picker (*apk* from *sac2000*) on the same data sets for comparison. For the Dead Sea dataset, about 67% picks are detected and picked within 0.5 sec of analyst picks, among which about 87% are within 0.2 sec of manual picks. The mean value and the standard deviation between the autopicks and manual picks are 0.023 and 0.133 sec, respectively. For the Parkfield dataset, about 87% of picks are detected and picked within 0.5 sec of manual picks, among which about 93% are within 0.1 sec of manual picks. The mean value and the standard deviation between the autopicks and manual picks are -0.03 and 0.068 sec, respectively. Thus, the W-AIC picker performs notably better than *apk* for the noisier Dead Sea dataset, whereas the performances are more comparable for the less noisy Parkfield dataset.

On the basis of these tests, we conclude that the W-AIC picker provides us an efficient and automatic way to pick *P*-wave arrivals. The picks obtained by the W-AIC picker can

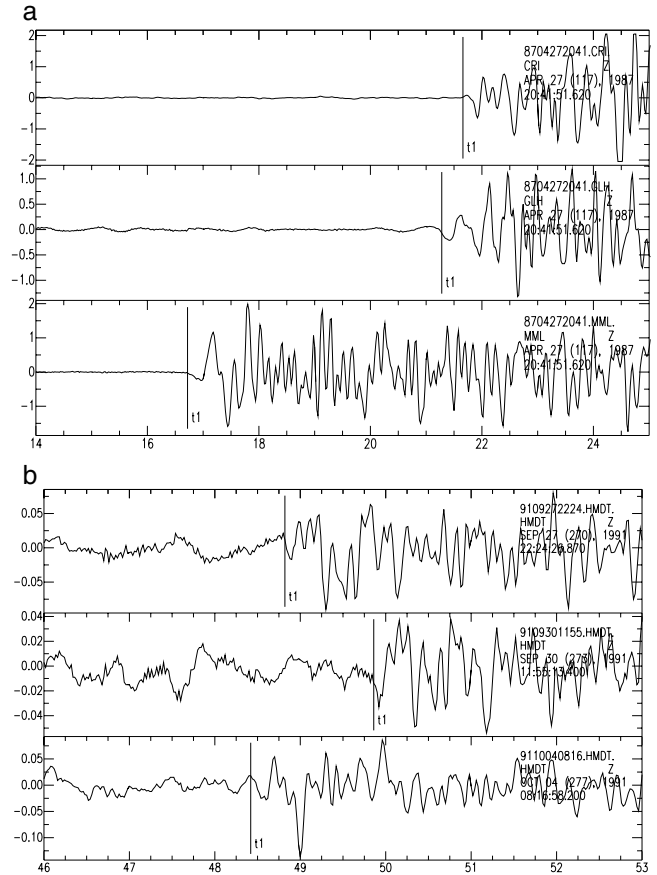


Figure 7. W-AIC picker applied to seismograms with (a) high S/N ratio and (b) low S/N ratio.

be treated as the preliminary picks for cross-correlation techniques. In this way, the picks can be further refined.

Conclusions

We developed an automatic *P*-phase picker based on the AIC combined with multiscale wavelet analysis. The *P*-wave arrival is a significant feature in a seismogram and will be retained over several scales, whereas random noise or other incoherent features will disappear quickly over larger scales. The AIC picker is applied directly to the absolute wavelet coefficients. If the picks at three scales are consistent, then a *P*-wave arrival is declared and the AIC picker is applied to the seismogram in the time window.

To reduce the noise in the seismogram, we apply the soft-thresholding scheme with the threshold chosen by application of the Birge-Massat penalization method to the wavelet coefficients. This approach is advantageous over the conventional bandpass-filtering method, which is more likely to distort the *P*-wave arrival or reduce its amplitude. In this way, the W-AIC picker is more robust in detecting the *P*-wave arrival even for noisy seismograms.

We tested this method on a set of seismic events from the Dead Sea region and Parkfield, California region. We

found that about 81% of the autopicks are within 0.2 sec of analyst picks for the Dead Sea dataset and about 93% of the autopicks are within 0.1 sec of analyst picks for the Parkfield dataset. In the cases that some spikes or glitches exist in the time window, the picker will erroneously claim that there is an arrival in the current time window. This problem can be corrected by applying a despiking algorithm before applying the W-AIC picker.

Acknowledgments

We are grateful to Bill Ellsworth for providing us his AIC program. We also thank two anonymous reviewers and associate editor Cezar Trifu for their constructive comments. H. Z. acknowledges British Petroleum for partial support of his graduate studies in Fall 2001. This research resulted from a project supported by the Defense Threat Reduction Agency (Contract DTRA01-01-C-0085), U.S. Department of Defense; the content does not necessarily reflect the position or the policy of the U.S. Government, and no official endorsement should be inferred.

References

- Akaike, H. (1973). Information theory and an extension of the maximum likelihood principle, in 2nd International Symposium on Information Theory, B. Petrov and F. Csaki (Editors), Budapest Akademiai Kiado, 267–281.
- Anant, S. K., and F. U. Dowla (1997). Wavelet transform methods for phase identification in three-component seismogram, *Bull. Seism. Soc. Am.* **87**, 1598–1612.
- Birge, L., and P. Massart (1997). From model selection to adaptive estimation, in *Festschrift for L. Le Cam*, D. Pollard, Editor, Springer, New York, 55–88.
- Chakra, A. B., and D. Okaya (1995). Frequency-time decomposition of seismic data using wavelet-based methods, *Geophysics* **60**, 1906–1916.
- Daubechies, I. (1992). Ten lectures on wavelets, in CBMS-NSF Regional Conference Series in Applied Mathematics, Vol. 61, Society for Industrial and Applied Mathematics, Philadelphia, Pennsylvania, 357 pp.
- Donoho, D. L. (1995). De-noising by soft-thresholding, *IEEE Trans. Inf. Theory* **41**, 613–627.
- Earle, P., and P. M. Shearer (1994). Characterization of global seismograms using an automatic-picking algorithm, *Bull. Seism. Soc. Am.* **84**, 366–376.
- Gendron, P., J. Ebel, and D. Manolakis (2000). Rapid joint detection and classification with wavelet bases via Bayes theorem, *Bull. Seism. Soc. Am.* **90**, 764–774.
- Goudswarrd, J., and K. Wapenaar (1998). Characterization of reflectors by multiscale amplitude and phase analysis of seismic data, *68th Ann. Int. Mtg. Soc. Expl. Geophys.*, 1688–1691.
- Goupillaud, P., A. Grossmann, and J. Morlet (1984). Cycle-octave and related transforms in seismic signal analysis, *Geoexploration* **23**, 85–102.
- Grossmann, A., and J. Morlet (1984). Decomposition of Hardy functions into square integrable wavelets of constant shape, *SIAM J. Math. Anal.* **15**, 723–736.
- Haykin, S. (1996). *Adaptive Filter Theory*, Prentice Hall, Upper Saddle River, New Jersey, 989 pp.
- Hsung, T.-C., D. P.-K. Lun, and W.-C. Siu (1999). Denoising by singularity detection, *IEEE Trans. Signal Processing* **47**, 3139–3144.
- Leonard, M. (2000). Comparison of manual and automatic onset time picking, *Bull. Seism. Soc. Am.* **90**, 1384–1390.
- Leonard, M., and B. L. N. Kennett (1999). Multi-component autoregressive techniques for the analysis of seismograms, *Phys. Earth Planet. Interiors* **113**, 247–264.
- Lervik, J. M., T. Rosten, and T. A. Ramstad (1996). Subband seismic data compression: optimization and evaluation, *IEEE Digital Signal Processing Workshop Proceedings*, 65–68.
- Maeda, N. (1985). A method for reading and checking phase times in auto-processing system of seismic wave data, *Zisin = Jishin* **38**, 365–379.
- Mallat, S. (1989). A theory for multiresolution signal decomposition: the wavelet representation, *IEEE Trans. Pattern Anal. Machine Intelligence* **11**, 674–693.
- Mallat, S., and W. L. Hwang (1992). Singularity detection and processing with wavelets, *IEEE Trans. Inform. Theory* **38**, 617–643.
- Sleeman, R., and T. van Eck (1999). Robust automatic P-phase picking: an on-line implementation in the analysis of broadband seismogram recordings, *Phys. Earth Planet. Interiors* **113**, 265–275.
- Strang, G., and T. Nguyen (1996). *Wavelets and Filter Banks*, Wellesley-Cambridge Press, Wellesley, Massachusetts, 490 pp.
- Tibuleac, I. M., and E. T. Herrin (1999). An automatic method for determination of Lg arrival times using wavelet transforms, *Seism. Res. Lett.* **70**, 577–595.
- Vidale, J. E. (1986). Complex polarization analysis of particle motion, *Bull. Seism. Soc. Am.* **76**, 1393–1405.
- Wickerhauser, M. V. (1994). *Adapted Wavelet Analysis from Theory to Software Algorithms*, A. K. Peters Ltd., Wellesley, Massachusetts, 504 pp.
- Withers, M., R. Aster, C. Young, J. Beiriger, M. Harris, S. Moore, and J. Trujillo (1998). A comparison of select trigger algorithms for automated global seismic phase and event detection, *Bull. Seism. Soc. Am.* **88**, 95–106.
- Wu, Y., and G. A. McMechan (1998). Wave extrapolation in the spatial wavelet domain with application to poststack reverse-time migration, *Geophysics* **63**, 580–600.

Department of Geology and Geophysics
University of Wisconsin–Madison
1215 W. Dayton Street
Madison, Wisconsin 53706
hjzhang@geology.wisc.edu

Manuscript received 6 December 2002.